Fraunhofer Institut
Techno- und
Wirtschaftsmathematik

J. Almquist, H. Schmidt, P. Lang, J. Deitmer,
M. Jirstrand, D. Prätzel-Wolters, H. Becker

Determination of interaction between MCT1 and CAII via a mathematical and physiological approach

Berichte des Fraunhofer ITWM, Nr. 136 (2008)

ISSN 1434-9973

Bericht 136 (2008)

Die Veröffentlichungen in der Berichtsreihe des Fraunhofer ITWM können bezogen werden über:

Fraunhofer-Institut für Techno- und
Wirtschaftsmathematik ITWM
Fraunhofer-Platz 1

67663 Kaiserslautern
Germany

Telefon: +49 (0) 6 31/3 16 00-0
Telefax: +49 (0) 6 31/3 16 00-10 99
E-Mail: info@itwm.fraunhofer.de
Internet: www.itwm.fraunhofer.de

Vorwort

Das Tätigkeitsfeld des Fraunhofer-Instituts für Techno- und Wirtschaftsmathematik ITWM umfasst anwendungsnahe Grundlagenforschung, angewandte Forschung sowie Beratung und kundenspezifische Lösungen auf allen Gebieten, die für Techno- und Wirtschaftsmathematik bedeutsam sind.

In der Reihe »Berichte des Fraunhofer ITWM« soll die Arbeit des Instituts kontinuierlich einer interessierten Öffentlichkeit in Industrie, Wirtschaft und Wissenschaft vorgestellt werden. Durch die enge Verzahnung mit dem Fachbereich Mathematik der Universität Kaiserslautern sowie durch zahlreiche Kooperationen mit internationalen Institutionen und Hochschulen in den Bereichen Ausbildung und Forschung ist ein großes Potenzial für Forschungsberichte vorhanden. In die Berichtreihe sollen sowohl hervorragende Diplom- und Projektarbeiten und Dissertationen als auch Forschungsberichte der Institutsmitarbeiter und Institutsgäste zu aktuellen Fragen der Techno- und Wirtschaftsmathematik aufgenommen werden.

Darüber hinaus bietet die Reihe ein Forum für die Berichterstattung über die zahlreichen Kooperationsprojekte des Instituts mit Partnern aus Industrie und Wirtschaft.

Berichterstattung heißt hier Dokumentation des Transfers aktueller Ergebnisse aus mathematischer Forschungs- und Entwicklungsarbeit in industrielle Anwendungen und Softwareprodukte – und umgekehrt, denn Probleme der Praxis generieren neue interessante mathematische Fragestellungen.

Prof. Dr. Dieter Prätzel-Wolters
Institutsleiter

Kaiserslautern, im Juni 2001

Determination of interaction between MCT1 and CAII via a mathematical and physiological approach

Joachim Almquist[1], Henning Schmidt[1†], Patrick Lang[2], Joachim W. Deitmer[3], Mats Jirstrand[1], Dieter Prätzel-Wolters[4], and Holger M. Becker[3‡]

[1]Fraunhofer-Chalmers Centre, Chalmers Science Park, SE-412 88 Göteborg, Sweden
[2]Abteilung "Systemanalyse, Prognose und Regelung", Fraunhofer Institut für Techno- und Wirtschaftsmathematik (ITWM), Fraunhofer-Platz 1, 67663 Kaiserslautern, Germany
[3]Division of General Zoology, Department Biology, University of Kaiserslautern, POB 30 49, D 67653 Kaiserslautern, Germany
[4]Technomathematik, University of Kaiserslautern, Erwin-Schroedingerstr., 67663 Kaiserslautern, Germany
[†]Present address: Systems Biology and Bioinformatics, Department of Computer Science, Universität Rostock, Albert Einstein Str. 21, 18051 Rostock
[‡]Corresponding author

Abstract

The enzyme carbonic anhydrase isoform II (CAII), catalysing the hydration and dehydration of CO_2, enhances transport activity of the monocarboxylate transporter isoform I (MCT1, SLC16A1) expressed in *Xenopus* oocytes by a mechanism that does not require CAII catalytic activity (Becker et al. (2005) J. Biol. Chem., 280). In the present study, we have investigated the mechanism of the CAII induced increase in transport activity by using electrophysiological techniques and a mathematical model of the MCT1 transport cycle. The model consists of six states arranged in cyclic fashion and features an ordered, mirror-symmetric, binding mechanism were binding and unbinding of the proton to the transport protein is considered to be the rate limiting step under physiological conditions. An explicit rate expression for the substrate flux is derived using model reduction techniques. By treating the pools of intra- and extracellular MCT1 substrates as dynamic states, the time dependent kinetics are obtained by integration using the derived expression for the substrate flux. The simulations were compared with experimental data obtained from MCT1-expressing oocytes injected with different amounts of CAII. The model suggests that CAII increases the effective rate constants of the proton reactions, possibly by working as a proton antenna.

Keywords: Mathematical modeling; Model reduction; Electrophysiology; pH-sensitive microelectrodes; Proton antenna

Introduction

Transport of acid/base equivalents across cell membranes plays a pivotal role both in intra- and extracellular pH regulation and for the import and export of metabolites, as many Na^+-dependent and Na^+-independent substrate transporters use H^+, OH^- or HCO_3^- as co- or counter-substrate. One family of these H^+-substrate cotransporters are the monocarboxylate transporters (MCT, SLC16) which comprise 14 isoforms. MCTs, that carry the energetic compounds lactate and pyruvate together with protons in an electroneutral 1 proton : 1 monocarboxylate stoichiometry, are expressed in most tissues, especially those with large energy consumption like muscle and brain (1, 2). In the brain, MCT1 is located mainly in glial cells, where it facilitates the export of lactate, which is then taken up by neurons via the high affinity MCT2; thereby the two isoforms are believed to shuttle lactate from glial cells to neurons, a mechanism that seems to be crucial for brain energy metabolism (3–7). In muscle, the predominant isoforms are MCT1, MCT3, and MCT4. MCT1 is highly expressed in oxidative type I fibers, while the density of MCT3 and MCT4 is independent of the fiber type (8–10). MCT3 and MCT4 seem to be responsible for the removal of lactate from glycolytic muscle cells, while MCT1 mediates lactate-import into oxidative fibers. Thereby the different isoforms facilitate lactate shuttling between glycolytic and oxidative muscle fibers (11). The transport of monocarboxylates between different cell types in the muscle and between muscle and blood has been found to have a significant impact on regulation of muscular pH (12–14). The isoform MCT1, used in the present study, has extensively been studied in different systems. MCT1 has a classical 12 transmembrane-helix structure, with both the N- and C-terminus being located intracellularly (15). Expression of MCT1 in *Xenopus* oocytes revealed a K_m value for lactate of 3.5 mM and a strong dependency of lactate transport from the extracellular H^+ concentration (16). Lactate transport via the MCTs has been described by different kinetic models. By measuring influx of ^{14}C-labeled lactate into red blood cells a kinetic model was proposed that describes the lactate transport as a symport system with ordered binding of lactate and H^+, in the sense that the proton binds first to the carrier, creating the binding site for the negatively charged lactate, followed by binding of lactate (17). After translocation of lactate and H^+ across the membrane, lactate is released first from the transporter followed by the proton. As the rates of monocarboxylate exchange are substantially faster than those of net transport, the return of the free carrier across the membrane was considered as the rate-limiting step for net lactic acid flux (18). Investigation of point mutations within critical residues of the MCT1 revealed that the proton is initially bound to D302 within the transmembrane helix 8 (TM 8). Lactate binds to R306 in TM 8. This binding interferes with proton binding at D302 and causes the proton to move to E369 in the loop between TM 10 and 11 which disrupts its interaction with R143 at TM 5 and causes the helices to rearrange (19). MCT1 has been shown to cooperate with the sodium-bicarbonate cotransporter NBCe1 (20), and with carbonic anhydrase isoform II (CAII) (21). Remarkably, the increase of MCT1 transport activity by CAII was independent of the catalytic activity which catalyzes the reaction between CO_2, H^+, and HCO_3^- (21). CAII seems to bind to, and enhance the activity of, various acid/base transporters like the sodium-bicarbonate cotransporter NBCe1 (22, 23), the chloride/bicarbonate exchanger AE1 (24) and the sodium/hydrogen exchanger NHE1 (25). In muscle cells, co-expression of CAII and acid/base transporting proteins like NBC, NHE1 and also the MCTs have been found to be pivotal in acid/base homeostasis (26). In addition it has been shown that extracellular carbonic anhydrase activity facilitates lactic acid transport in rat skeletal muscle fibers (27).

In the brain CAII is highly expressed in astrocytes where it plays a supportive role in pH regulation (28) and in lactate shuttling between astrocytes and neurons (29).

In the present study, we present a mathematical model based on rate equations and model reduction that describes H^+-lactate cotransport via the MCT1 and gives an explanation of the mechanism by which CAII increases MCT1 activity. H^+-lactate cotransport via the MCT1 can be described as a multi-step process including substrate binding, translocation of bound substrate over the membrane, and substrate release (30). This chain of events can be described by a number of states, representing a protein or protein-substrate complex with its binding sites or bound substrates facing either the intracellular or extracellular side of the membrane. At any given time, a single protein belongs to precisely one of these states, but the total population of MCT1 proteins are divided into sub-populations distributed over all the different states. If the number of proteins residing in every state is sufficiently large, the rate of change of each state can be described by a deterministic, ordinary differential equation (ODE) based on mass action kinetics (31, 32). The set of all rate equations, then, constitutes the model of the membrane transport process. Model reduction is a way of simplifying models to reach an appropriate level of details for experimental validation (30, 31). Based on the transport measurement techniques used in this study, it is not possible to determine the values of all rate constants appearing in the type of ODE model described above. It is therefore desirable to reduce unnecessary complexity of the model. Two common methods of reducing the number of ODEs, both based on timescale separation, are the quasi-equilibrium approximation and the quasi-steady-state approximation (31, 33). By distinguishing between fast and slow reactions in the ODE system, two or more states interconnected by fast reactions can be treated by the quasi-equilibrium approximation on the timescale of the slower reactions. Mathematically, this can be formulated as an algebraic constraint for each fast reaction. For a cyclic chain of n states, it is at most possible to find $n-1$ independent constraints from fast reactions. Depending on the number of slow reactions it could be fewer. All states in the system, even those linked to "slow" reactions, reach their steady state a lot faster than relevant changes in substrate concentrations. This is a consequence of the fact that substrates are present in numbers of $10^{14} - 10^{15}$ molecules while there are an estimated number of 10^{10} MCT1 proteins (Stefan Bröer, personal communication). On the timescale of relevant changes in substrate concentrations, it is therefore reasonable to consider the subsets of quasi-equilibrium interconnected states, connected by the slower reactions, to be in quasi-steady-state. This will provide additional algebraic constraints. If one can find as many linearly independent constraints as there are numbers of states, it is possible to solve for a unique solution of occupancy level of all states. Once this task is achieved, the dynamic, multi-state description of the system can be reduced to an explicit, analytic rate expression for the trans-membrane transport of substrates, being a function of slow rate constants, equilibrium constants, and substrate concentrations. This is a much more general way of characterizing the transport process than merely stating a V_{max} and an apparent K_m. The substrate transport rate expression gained from the model reduction can then be used to describe the rate of change of substrate concentrations, taking place on the slowest of all timescales .

Materials & Methods

Constructs, oocytes and injection of cRNA and carbonic anhydrase

Rat MCT1 cDNA (MCT1) cloned in oocyte expression vector pGEM-He-Juel, which contains the 5' and the 3' untranscribed regions of the *Xenopus* β-globulin flanking the multiple cloning site, was kindly provided by Dr. Stefan Bröer, Canberra (34). Plasmid DNA was linearised with NotI and transcribed *in vitro* with T7 RNA-Polymerase in the presence of the cap analogon m7G(5')ppp(5')G (mMessage mMachine, Ambion Inc., USA) to produce a capped RNA transcript. The cRNA was purified with the Qiagen RNeasy MinElute Cleanup Kit (Qiagen GmbH, Hilden, Germany) and stored at -80℃ in DEPC-H_2O. *Xenopus laevis* females were purchased from Xenopus Express Inc. (Vernassal, France). Oocytes were isolated and singularized by collagenase (Collagenase A, Roche, Mannheim, Germany) treatment in Ca^{2+}-free oocyte saline at 28℃ for 2h. The singularized oocytes were left overnight in an incubator at 18℃ in Ca^{2+}-containing oocyte saline (pH 7.8) to recover. The oocyte saline had the following composition (in mM): NaCl, 82.5; KCl, 2.5; $CaCl_2$, 1; $MgCl_2$, 1, Na_2HPO_4; 1, HEPES, 5, titrated with NaOH to the desired pH. In the bicarbonate-containing saline, NaCl was replaced by an equivalent amount of $NaHCO_3$ and the solution was aerated with 5% CO_2. Oocytes of the stages V and VI were selected and injected with 7 ng of MCT1-cRNA dissolved in DEPC-H_2O using glass micropipettes and a microinjection device (Nanoliter 2000, World Precision Instruments, Berlin, Germany). Control oocytes were injected with an equivalent volume of DEPC-H_2O. 50, 200 or 500 ng of CAII, isolated from bovine erythrocytes (C3934, Sigma-Aldrich, Taufkirchen, Germany), dissolved in 25 nl DEPC-H_2O, were injected 20-24 h before electrophysiological measurement. Control oocytes were injected with 25 nl DEPC-H_2O.

Intracellular pH measurements

For measurement of intracellular pH (pH_i) and membrane potential double-barreled microelectrodes were used; the manufacture and application have been described in detail previously (35). Briefly, for double-barreled microelectrodes, two borosilicate glass capillaries of 1.0 and 1.5 mm in diameter were twisted together and pulled to a micropipette. The ion-selective barrel was silanized with a drop of 5% tri-N-butylchlorsilane in 99.9% pure carbon tetrachloride, backfilled into the tip. The micropipette was baked for 4.5 min at 450℃ on a hot plate. H^+-sensitive cocktail (Fluka 95291, Fluka, Buchs, Switzerland) was backfilled into the tip of the silanized ion-selective barrel and filled up with 0.1 M Na-citrate, pH 6.0. The reference barrel was filled with 3 M KCl. To increase the opening of the electrode-tip, it was bevelled with a jet stream of aluminium powder suspended in H_2O. Calibration of the electrodes was carried out in oocyte salines by changing the pH by 0.6 units. The central and the reference barrel of the electrodes were connected by chlorided silver wires to the headstages of an electrometer amplifier. Electrodes were accepted for use in the experiments, when their response exceeded 50 mV per unit change in pH; on average, they responded with 54 mV for unit change in pH. As described previously (16), optimal pH changes were detected when the electrode was located near the inner surface of the plasma membrane. This was achieved by carefully rotating the oocyte with the impaled electrode. All experiments were carried out at room temperature.

Calculation of $[H^+]_i$

The measurements of pH_i were stored digitally using homemade PC software based on the program LabView (National Instruments Germany GmbH, München, Germany) and were routinely converted into intracellular H^+ concentration, $[H^+]_i$. Thus, changes in the $[H^+]_i$ are recorded, which take into account the different pH baseline, as e.g. measured in HEPES- and CO_2/HCO_3^--buffered salines, see also (20). The rate of change of the measured $[H^+]_i$ was analyzed by determining the slope of a linear regression fit using the spread sheet program OriginPro 7 (OriginLab Corporation, Northampten, USA).

Voltage-Clamp recording

A borosilicate glass capillary, 1.5 mm in diameter, was pulled to a micropipette and backfilled with 3 M KCl. The resistance of the electrodes measured in oocyte saline was around 1 M. For voltage-clamp, the electrode was connected to the head-stage of an Axoclamp 2B amplifier (Axon Instruments, USA). The experimental bath was grounded with a chlorided silver wire coated by agar dissolved in oocyte saline. Oocytes were clamped to a holding potential of -40 mV.

Calculation of statistics

Statistical values are presented as means and standard errors of the means (S.E.M.). For calculation of significance in differences, Students *t*-test or, if possible, a paired *t*-test was used.

Mathematics and modeling

Given the cell volume, a derived rate expression can be used to calculate the changes in intracellular substrate concentration, induced by changes in the substrate gradient. The complexity of the rate expression requires that this must be done by numeric integration. In addition to the changes in substrate concentrations related to membrane transport, it is also important to consider changes in concentrations due to other chemical reactions in the cytosol bulk. Lactate has a rather low pK_a value of 3.86. Since the experiments are carried out at extracellular pH (pH_o) 5 to 8, the only species considered is the dissociated acid form. Protons on the other hand, must receive special treatment because of their strong linkage with buffers. The intrinsic buffer system of the oocyte is modeled as a single species with a single pK_a, $B^- + H^+ \rightleftharpoons HB$. Buffering is assumed to be instantaneous, and the pK_a is such that the buffer never saturates. The extracellular space is not a dynamic compartment in the same sense as the intracellular space. Perfusion of the bath solution maintains a constant, controlled environment around the oocyte. For this reason, the extracellular space was used as a signal input compartment reflecting the experiment protocol. To make the model more realistic, switching of the bath solution is modeled as a first order system with some time constant. This time constant can be measured directly, preferably at the same time as the electrodes are being calibrated.

The Systems Biology Toolbox for MATLAB (36) was used to create the cell model and to perform the numerical integrations, together with the extension package SBaddon (37). The toolbox features several modeling and simulation tools and a special representation of the experiment protocols. The $\Delta H^+/\Delta t$ following input signals was extracted from simulated

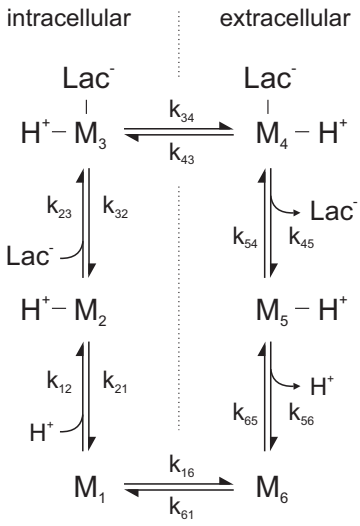

Figure 1: **Kinetic model of H^+-lactate co-transport via the MCT1.** M_1 to M_6 represent the six states of MCT1 during substrate transport, k_{xy} gives the rate constants between two transporter states.

time series, and then compared to real measurements. The analytic solution of systems of algebraic equations were obtained with Mathematica (Wolfram Research, Inc.).

Results

The aim of this study was to determine the mechanism of the monocarboxylate transporter (MCT1) and how it interacts with the enzyme carbonic anhydrase II (CAII), based on a combination of electrophysiological techniques and mathematical modeling. The transport process of MCT1 was modeled as a number of interconnected states, representing a network of discrete protein-substrate configurations. Fig. 1 shows a hypothetical model of this type for the MCT1 transport. Each of the six MCT1-states, indicated by an M with an index, represents the protein or a protein-substrate complex. An efflux transport cycle starts with an intracellular proton binding to the MCT1, M_1, causing a transition to M_2. After binding of lactate the protein-substrate complex moves from M_3 to M_4, making the substrates face the extracellular side. The substrates then dissociates from the protein in a reversed order through M_5 and M_6, before the translocation of the binding-sites to M_1, completing the cycle. Since all reactions are reversible, the exact behavior of an individual MCT1 molecule can not be calculated. Therefore the model describes the state transitions by a large population of proteins.

The rate of change of each state in Fig. 1 is described by an ordinary differential equation

$$\frac{d}{dt}M_1 = k_{21}M_2 + k_{61}M_6 - k_{12}[H^+_{in}]M_1 - k_{16}M_1 \tag{1}$$

$$\frac{d}{dt}M_2 = k_{12}[H^+_{in}]M_1 + k_{32}M_3 - k_{21}M_2 - k_{23}[Lac^-_{in}]M_2 \tag{2}$$

$$\frac{d}{dt}M_3 = k_{23}[Lac^-_{in}]M_2 + k_{43}M_4 - k_{32}M_3 - k_{34}M_3 \tag{3}$$

$$\frac{d}{dt}M_4 = k_{34}M_3 + k_{54}[Lac^-_{ex}]M_5 - k_{43}M_4 - k_{45}M_4 \tag{4}$$

$$\frac{d}{dt}M_5 = k_{45}M_4 + k_{65}[H^+_{ex}]M_6 - k_{54}[Lac^-_{ex}]M_5 - k_{56}M_5 \tag{5}$$

$$\frac{d}{dt}M_6 = k_{16}M_1 + k_{56}M_5 - k_{61}M_6 - k_{65}[H^+_{ex}]M_6 \tag{6}$$

The dynamics of this system will be influenced by the relative speed of the reactions. By assuming that one or several of the reactions are slower than the others, the remaining reactions can, by the quasi-equilibrium approximation, be considered to always be in equilibrium. To illustrate how the model reduction is done in practice, we assume that the reactions between M_1 and M_2, and between M_5 and M_6, are slower than the other reactions. This assumption yields four quasi-equilibrium constraints for the system

$$k_{16}M_1 = k_{61}M_6 \tag{7}$$

$$k_{34}M_3 = k_{43}M_4 \tag{8}$$

$$k_{23}[Lac^-_{in}]M_2 = k_{32}M_3 \tag{9}$$

$$k_{54}[Lac^-_{ex}]M_5 = k_{45}M_4 \tag{10}$$

where we introduce the notation $K_i = k_{23}/k_{32}$, $K_o = k_{54}/k_{45}$, $K_l = k_{34}/k_{43}$, and $K_e = k_{61}/k_{16}$ for later convenience. Also assuming that the total number of proteins are constant over time, i.e.,

$$\sum_i M_i = M_{tot} \tag{11}$$

and that the subsets of quasi-equilibrium states are in quasi-steady-state,

$$k_{12}[H^+_{in}]M_1 - k_{21}M_2 = k_{56}M_5 - k_{65}[H^+_{ex}]M_6 \tag{12}$$

gives a total of six independent algebraic constraints. Solving the system of linear equations Eq. 7-12 yields a distribution M^s of the MCT1s over the six states as a function of the intra and extracellular concentrations of protons and lactate. The rate of net flux over the membrane is then given by

$$T = k_{12}[H^+_{in}]M^s_1 - k_{21}M^s_2 \tag{13}$$

or equivalently

$$T = k_{56}M^s_5 - k_{65}[H^+_{ex}]M^s_6 \tag{14}$$

These two expressions are equivalent because of the constraint in Eq. 12. With the solution of Eq. 7-12 inserted into Eq. 13 or Eq. 14, the expression for the net transport becomes

$$T = M_{tot}\frac{k_{12}k_{56}K_iK_l[H^+_{in}][Lac^-_{in}] - k_{21}k_{65}K_oK_e[H^+_{ex}][Lac^-_{ex}]}{A[H^+_{in}] + B[H^+_{ex}] + C[Lac^-_{in}] + D[Lac^-_{ex}]} \tag{15}$$

where A, B, C and D are given by

$$A = k_{12}(K_iK_l[Lac^-_{in}] + K_o[Lac^-_{ex}] + K_iK_o(K_l+1)[Lac^-_{in}][Lac^-_{ex}]) \tag{16}$$

$$B = k_{65}(K_iK_eK_l[Lac^-_{in}] + K_oK_e[Lac^-_{ex}] + K_iK_oK_e(K_l+1)[Lac^-_{in}][Lac^-_{ex}]) \tag{17}$$

$$C = k_{56}K_iK_l(K_e+1) \tag{18}$$

$$D = k_{21}K_o(K_e+1) \tag{19}$$

As a consequence of the second law of thermodynamics, the rate and equilibrium constants in Eq. 15 must obey the following equation.

$$k_{12}k_{56}K_iK_l = k_{21}k_{65}K_oK_e \tag{20}$$

Other combinations of substrate binding-order and assumptions about slow reactions lead, in a similar way, to rate expressions of different functional form. To find the best description of the system, the set of these combinations must be explored. As possible rate-limiting steps, we consider the binding and release of protons, the binding and release of lactate, the translocation of the loaded carrier, and the translocation of the empty carrier. As possible binding orders, we consider only the two types with mirror-symmetric binding (first in, last out). This gives eight candidate models. The omission of glide-symmetry and none-ordered binding (random binding) is discussed later.

In order to discriminate between the different models we measured the change in intracellular H^+ concentration, as an indicator for transport activity, in MCT1 expressing oocytes during efflux of H^+ and lactate. The efflux experiment was chosen in order to control the composition of the *trans*-side solution via the extracellular bath. By using a bath solution without lactate, or with lactate but at a very high pH, a situation with practically only one of the two substrates present was created. In the models, this corresponds to setting either $[Lac^-_{ex}]$ or $[H^+_{ex}]$ to zero. A thorough analysis of the considered models reveals that some of them show an efflux transport rate which is dependent on the extracellular substrate not removed. This means that in some model configurations, a single substrate on the *trans*-side may act as an inhibitor of transport. Tab. 1 shows possible single substrate inhibitions for the different model configurations. All model configurations are sensitive to one of the substrates, except for two configurations that predict inhibition features for both protons and lactate. This suggests that certain model configurations can be ruled out on the basis of single substrate inhibition experiments.

To discriminate between the different models, we measured efflux of H^+ in a MCT1 expressing oocyte under different conditions as shown in Fig. 2. The cell was loaded with 3 mM lactate at an external pH (pH_o) of 7.0. After equilibrium was reached, the extracellular solution was changed either to 0 mM lactate, pH_o 9.0 (Fig. 2A), 60 mM lactate, pH_o 9.0 (Fig. 2B), or 0 mM lactate pH_o 6.0 (Fig. 2C). The experiment was repeated three times with the same results. Loading of lactate resulted in an intracellular acidification that reached a

Assumed properties of transport kinetics		Predicted effect on transport	
First in, last out	Rate-limiting step	Inhibition by H^+	Inhibition by Lac^-
Proton (H^+)	binding/release of H^+	Yes	Yes
	binding/release of Lac^-	Yes	No
	translocation of empty carrier	Yes	No
	translocation of loaded carrier	Yes	No
Lactate (Lac^-)	binding/release of H^+	No	Yes
	binding/release of Lac^-	Yes	Yes
	translocation of empty carrier	No	Yes
	translocation of loaded carrier	No	Yes

Table 1: Single substrate inhibitions for the different model configurations.

plateau at an intracellular pH (pH_i) of 7.3, which equals an $[H^+]_i$ of 50 nM. From this value an intracellular lactate concentration of 6 mM can be calculated from the Donnan equation. Simultaneously removing both substrates by changing extracellular solution to 0 mM lactate, 1 nM H^+ (pH_o 9.0) resulted in a fast intracellular alkalinization with a rate of -20.3 nM H^+/min (Fig. 2A), induced by export of lactate and H^+ via the MCT1. Decreasing the extracellular H^+ concentration to 1 nM and simultaneously increasing the lactate concentration to 60 mM, resulted in slow substrate efflux with a rate of -5.7 nM H^+/min (Fig. 2B). In the same way, removal of lactate during increase of H^+ concentration to 1 μM (pH_o 6.0) resulted in a weak intracellular alkalinization with a rate of -2.4 nM H^+/min (Fig. 2C). It appears that the presence of a single extracellular MCT1 substrate, either protons or lactate, is sufficient to substantially decrease the rate of efflux.

According to the kinetic analysis summarized in Tab. 1, the results in Fig. 2 indicate two possible model configurations. It is either the case where the proton is the first substrate to bind to MCT1, and where the H^+ binding/release is also the slowest step, or the reversed case where lactate is the first substrate that binds to MCT1, and where the lactate binding/release is the slowest step. However, since MCT1 is prone to *trans*-acceleration (18), the latter case could be discarded. Thus, in our description of MCT1 transport, we adopt the model consisting of the binding scheme in Fig. 1 with the two proton reactions being the rate-limiting steps. Consequently, MCT1 transport will be described by Eq. 14. As well as describing MCT1 transport as such, Eq. 14 is the starting point for modeling the interaction between MCT1 and CAII.

CAII is believed to enhance transport activity of MCT1 either by removing H^+ from the transporter pore or supplying the transporter with H^+ via a proton shuttle along a chain of CAII at the cells inner membrane surface and an enhanced exchange of H^+ with the cytosol (Becker & Deitmer, unpublished), taking direct influence on the rate of proton binding and release at the MCT1. Since the binding and release of the proton are the only reactions in the model that are not constantly in equilibrium, a change in the corresponding rate constants could change the transport rate without altering the equilibrium. Additionally, it has to be taken into consideration that CAII only is present intracellularly, which makes any effect on k_{56} and k_{65} unlikely. As a consequence, interaction between MCT1 and CAII will be modeled as a more efficient way of proton exchange between the cytosol bulk and the MCT1 proton target site. Both k_{12} and k_{21} are increased with a factor g_{CA}, representing the effect of CAII.

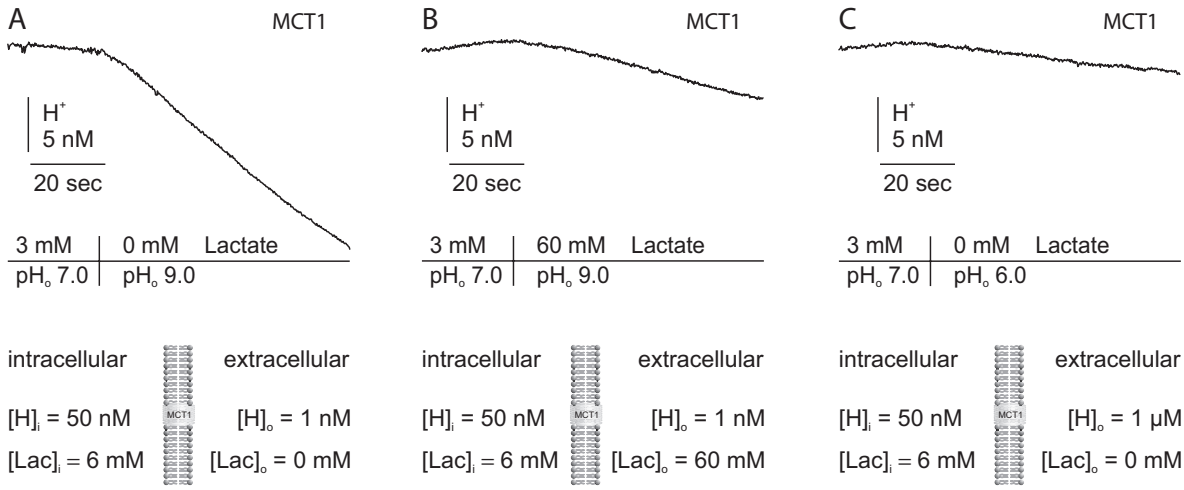

Figure 2: **Proton efflux via the MCT1 as subject to extracellular H^+ and lactate.** A MCT1 expressing oocyte was loaded with 3 mM lactate at pH_o 7.0. After equilibrium was reached extracellular solution was either changed to 0 lactate, pH_o 9.0 (**A**), 60 mM lactate, pH_o 9.0 (**B**) or 0 mM lactate, pH_o 6.0 (**C**). Shown is the intracellular H^+ concentration shortly before and during change in extracellular solution. The sketches under the original recordings show the intra- and extracellular concentration of lactate and H^+ at the point of change in extracellular solution.

In the case with no CAII, g_{CA} was set to one. The model reduction procedure was repeated with Eq. 12 replaced with

$$g_{CA}k_{12}[H^+_{in}]M_1 - g_{CA}k_{21}M_2 = k_{56}M_5 - k_{65}[H^+_{ex}]M_6 \tag{21}$$

which leads to a new rate expression including the impact of CAII in which the parameters must still obey Eq. 20.

$$T_{CA} = g_{CA}M_{tot}\frac{k_{12}k_{56}K_iK_l[H^+_{in}][Lac^-_{in}] - k_{21}k_{65}K_oK_e[H^+_{ex}][Lac^-_{ex}]}{A'[H^+_{in}] + B[H^+_{ex}] + C[Lac^-_{in}] + D'[Lac^-_{ex}]} \tag{22}$$

where B and C are the same as before, but with A and D replaced with A' and D' now including the g_{CA} factor

$$A' = g_{CA}k_{12}(K_iK_l[Lac^-_{in}] + K_o[Lac^-_{ex}] + K_iK_o(K_l+1)[Lac^-_{in}][Lac^-_{ex}]) \tag{23}$$

$$D' = g_{CA}k_{21}K_o(K_e+1) \tag{24}$$

Hence, g_{CA} now appears both in the numerator and in some of the terms in the denominator. Thus, the effect of making g_{CA} larger than one will depend on the proportions of the denominator terms. If the terms containing g_{CA} are dominating, the effect of increasing g_{CA} will be small. On the other hand, if the terms not containing g_{CA} are dominating, increasing g_{CA} will lead to an significant increase in the total transport rate.

The rate expression in Eq. 22 can now be compared to the data of an efflux experiment with no lactate at the outside, referred to as zero-*trans* efflux experiment. MCT1 expressing

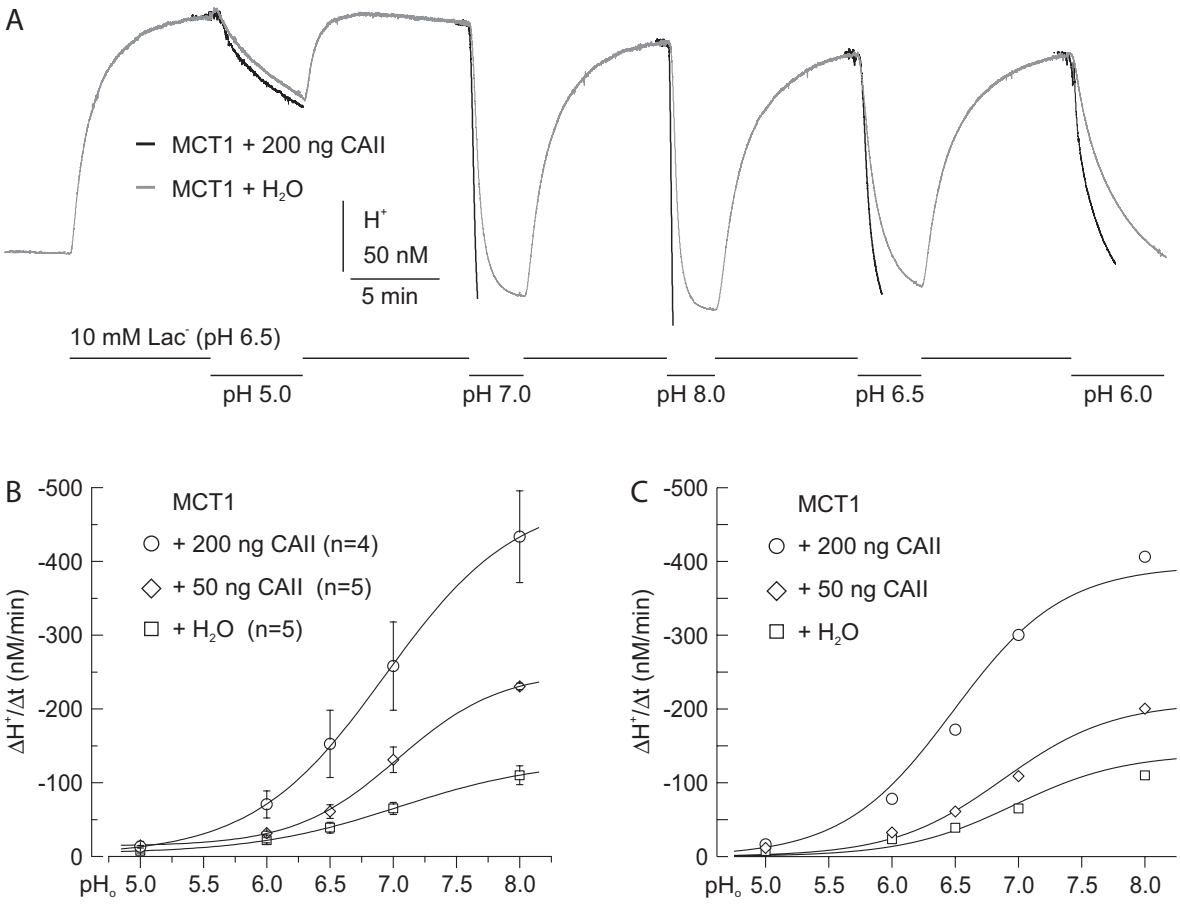

Figure 3: **Dependency of H^+-efflux on extracellular H^+ concentration.** (**A**) Original recordings of the intracellular H^+ concentration in MCT1-expressing oocytes injected either with 50 ng of CAII (black trace) or H_2O (gray trace), respectively, during application of 10 mM lactate in HEPES buffered solution at pH_o 6.5 followed by removal of lactate at extracellular pH of 5.0, 6.0, 7.0, and 8.0, respectively. (**B**) Rate of change in intracellular H^+ concentration in MCT1-expressing oocytes injected either with CAII (50 or 200 ng) or H_2O as induced by removal of 10 mM lactate at varying extracellular pH. (**C**) Simulation of the rate of change in intracellular H^+ concentration in MCT1-expressing oocytes with varying concentrations of CAII as induced by removal of 10 mM lactate at varying extracellular pH.

oocytes, either injected with 50 or 200 ng of CAII, or an equivalent volume of H_2O were loaded with 10 mM lactate at a pH_o of 6.5. After equilibrium was reached, lactate was removed and pH_o was changed to a value between 5.0 and 8.0. Fig. 3A shows the original recordings of the intracellular H^+ concentration of MCT1 expressing oocytes either injected with 200 ng of CAII (black trace) or H_2O (grey trace). The values of the measurements are given in Fig. 3B. Changes in intracellular H^+ concentration during removal of lactate are plotted against the extracellular pH value. Injection of CAII leads to an increase in the rate of change in intracellular H^+ concentration ($\Delta H^+/\Delta t$). The magnitude of the increase grows for higher extracellular pH, but the relative increase stays at a similar level throughout the whole pH-range. The increase in transport activity was further amplified by an increased concentration

of injected CAII. For modeling the zero-*trans* efflux experiment offers the advantage that substrate concentrations on the *trans*-side are kept constant because the bath solution is continuously replaced, which prevents any accumulation of lactate on the *trans*-side. Putting $[Lac^-_{ex}]$ to zero, Eq. 22 reduces to

$$T_{CA} = g_{CA} M_{tot} \frac{k_{12} k_{56} [H^+_{in}]}{g_{CA} k_{12} [H^+_{in}] + k_{65} K_e [H^+_{ex}] + k_{56}(K_e + 1)} \tag{25}$$

Interestingly, this rate is independent of the intracellular lactate concentration. To obtain the initial rate of efflux following a change in the bath solution, it is sufficient to insert the known values of intra and extracellular pH. Fig. 3C shows the calculated pH_o dependence of Eq. 25 together with the data points from Fig. 3B. The parameters k_{12} and k_{65} are assumed to be $4 \times 10^7 \mathrm{mM^{-1}s^{-1}}$, corresponding to diffusion-limited protonation (38). A best fit to data was found for $k_{56} = 2.6 \times 10^3 \mathrm{s^{-1}}$, $K_e = 4.5$, and $g_{CA} = 1$, 2, and 5 for 0, 50, and 200 ng of CAII, respectively.

To further investigate the effect of extracellular pH on the CAII induced increase in MCT1 transport activity, we measured the change in intracellular H^+ concentration in MCT1-expressing oocytes, either injected with 50 ng of CAII or an equivalent amount of H_2O, during application of 10 mM lactate at different extracellular pH values between 6.0 and 8.0 (Fig. 4A). Transport activity of MCT1 was determined by measuring $\Delta H^+/\Delta t$. Both for CAII injected as well as for H_2O injected oocytes a decrease in extracellular pH resulted in an increase in MCT1 transport activity. Injection of CAII augmented pH dependency of MCT1 transport activity, increasing $\Delta H^+/\Delta t$ to a bigger extent at low extracellular pH values, while at high pH_o only a small CAII induced increase in MCT1 activity could be observed (Fig. 4C). The injection of CAII lead to a more sigmoid shaped curve, compared to the curve observed in MCT1 expressing oocytes without CAII. Fig. 4B shows the simulation of the experiment as described in Fig. 4A. The initial flux rates from the simulation are shown in Fig. 4D. Even though the experiment starts from zero-*trans* conditions, substrates will continuously accumulate in the cell. For large fluxes, accumulation is so rapid that even during the 20 s time interval where the lactate induced acidification shows a nearly linear kinetics, which is used to measure $\Delta H^+/\Delta t$, a counter-flow may have developed. This motivates the use of Eq. 22 in the simulations. The parameter values used to fit the data were $K_i = K_o = 0.5 \mathrm{mM^{-1}}$, $K_e = K_l = 4.5$, $k_{56} = k_{21} = 1 \times 10^3 \mathrm{s^{-1}}$, and $g_{CA} = 4$, showing a somewhat lower value of k_{56} and a higher value of g_{CA} compared to the simulations in Fig. 3. The simulated rate of substrate influx for CAII-injected cells comes in two variants. One where the cells buffer capacity is decreased compared to cells without CAII (black trace), and one where the buffer capacity is left unchanged at the level of H_2O cells (dotted curve). The former fits the data of the measurements shown in Fig. 4C better, but the latter illustrates the properties of the model more clearly. Nevertheless, in both cases CAII induced enhancement of inward transport has a strong dependence on extracellular pH. For higher pH_o the percental increase in transport rate is smaller than for lower pH_o. As the dotted and grey traces only differ by g_{CA}, this emphasizes the effect of CAII unclouded by putative differences in oocyte batches. In a former study it has been shown that at pH_o 7.5 nearly no CAII induced increase in MCT1 expressing oocytes could be observed, while at pH_o 6.0 a strong effect occurred (Becker & Deitmer, unpublished).

Finally, the effect of different extracellular concentrations of lactate was investigated by influx experiments. Fig. 5A shows the original recordings of intracellular H^+ concentration

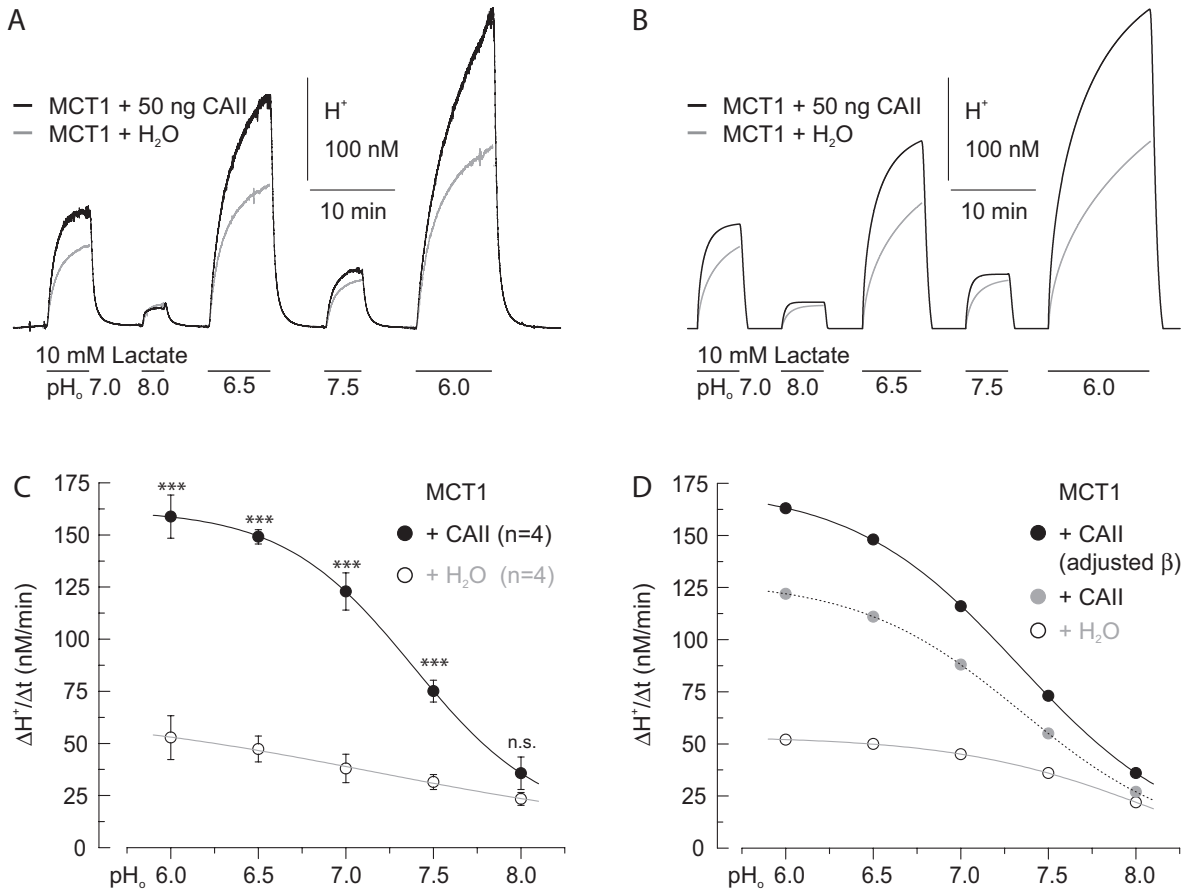

Figure 4: **Dependency of H^+-influx on extracellular H^+ concentration.** (**A**) Original recordings of the intracellular H^+ concentration and (**B**) simulation of the changes in intracellular H^+ concentration in MCT1-expressing oocytes injected either with 50 ng of CAII (black trace) or H_2O (gray trace), respectively, during application of 10 mM lactate in HEPES buffered solution at pH_o 6.0, 6.5, 7, 7.5, and 8.0, respectively. (**C**) Rate of rise in intracellular H^+ concentration in MCT1-expressing oocytes injected either with 50 ng of CAII or H_2O as induced by application of 10 mM lactate at varying extracellular pH. (**D**) Simulation of the rate of rise in intracellular H^+ concentration in MCT1-expressing oocytes with varying concentrations of CAII as induced by application of 10 mM lactate at varying extracellular pH.

of two MCT1 expressing oocytes, either injected with 50 ng of CAII (black trace) or H_2O (grey trace) during application of lactate at very low and high concentration (0.3 mM and 10 mM) at low and high extracellular pH (pH_o 6.0 and pH_o 7.5). The measurements indicate that the increase in transport activity induced by CAII is most evident at pH_o 6.0, and only marginal at pH_o 7.5. The concentration of lactate does not seem to affect the CAII dependent enhancement of MCT1 transport. Intracellular resting pH of MCT1-expressing oocytes injected with CAII or H_2O were 7.38±0.03 and 7.33±0.02, respectively (Becker & Deitmer, unpublished). Fig. 5B shows the simulation of the experiment as described in Fig. 5A with the same parameters as in Fig. 4.

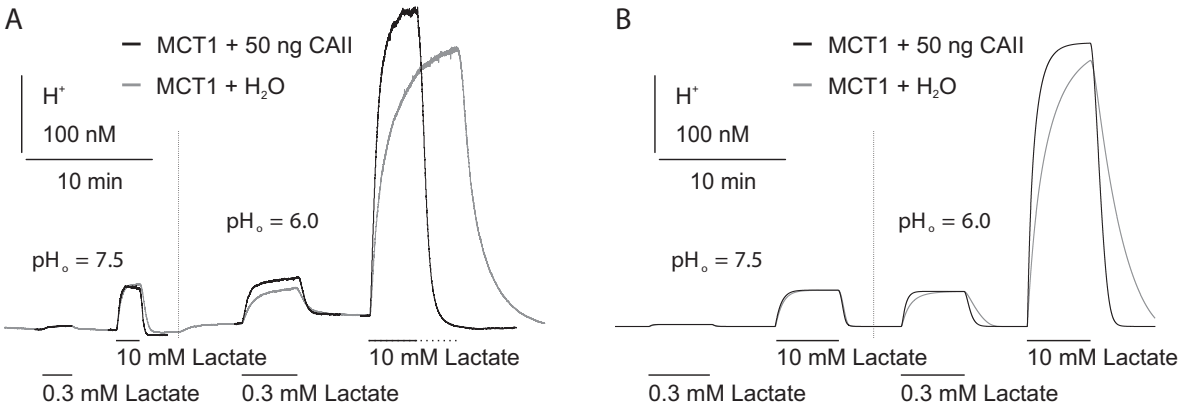

Figure 5: **Dependency of MCT1 transport activity on substrate concentration.** (**A**) Original recordings of the intracellular H^+ concentration and (**B**) simulation of the changes in intracellular H^+ concentration in MCT1-expressing oocytes injected with 50 ng of CAII (black trace) or H_2O (gray trace), respectively, during application of 0.3 and 10 mM lactate in HEPES buffered solution at pH_o 7.5 and 6.0.

Discussion

In the present study we investigated transport function of the MCT1 and its interaction with the enzyme CAII by means of electrophysiological measurements of MCT1 activity in *Xenopus* oocytes and by mathematical modeling of the transport process. Viewing the transport process as a series of sub-steps, assumptions about which step is the rate-limiting one will play a crucial role in the resulting kinetics. Based on single substrate inhibition experiments we propose, that association, and dissociation, of the proton is the step that limits the turnover-rate of the symport. These findings are in contrast to earlier studies stating that the translocation of the empty carrier is the rate-limiting step (1, 39). However, combining the assumption of H^+ binding and release being the rate-limiting step with the previously suggested ordered binding scheme, where the proton binds in, and is released, first (17), is still compatible with the fast exchange experiments carried out earlier (39) and the single substrate inhibition, but opens up a natural role for CAII as an accelerator of proton reactions. When testing the impact of different binding order schemes on the reduced rate expression, some configurations that sometimes appear in similar studies were omitted. Glide symmetry, the opposite of mirror symmetry, means that the substrate that binds first is also released first. Since the conclusion that the proton binding/release is the slowest step does not depend on the intracellular binding order, glide symmetry could not be ruled out by the single substrate inhibition experiments used in this study. However, any model where substrate binding/release is rate-limiting means that glide symmetry must be ruled out on the basis of the accelerated exchanges experiments (39). Another binding mechanism often considered is the so called random binding (40, 41). Here, either substrate may be first to bind or first to be released, determined by some probabilistic mechanism. Based on the measurements in this study, random binding cannot be excluded as a possible mechanism. Nevertheless, this is not surprising since all ordered binding schemes are just special cases of the more general random binding.

The main results of this study are the binding order scheme in Fig. 1 and the rate

expression in Eq. 22. The implications of these results can be summarized as follows. During net transport of protons and lactate via the MCT1, the proteins must pass through two bottleneck reactions, the binding and release of protons on both sides of the membrane. Depending on the substrate concentrations and the parameters of the model, one of these bottlenecks may be dominating. For the special cases of zero-*trans* influx or efflux (setting $[Lac^-_{in}]$ or $[Lac^-_{ex}]$ to zero in Eq. 22), this will be determined by the pH at both sides of the membrane, the rate constants for the proton binding/release, and any bias towards intra or extracellular location of the empty carrier. If the bottleneck should be between states M_1 and M_2, the presence of CAII will have an enhancing effect on transport. In the efflux experiments, CAII has a similar sized effect over the whole range of pH_o. Here, the intracellular binding and release of protons limits the process irrespectively of pH_o, a consequence of the asymmetric distribution of empty carriers ($K_e = 4.5$). For the influx of substrate via the MCT1 on the other hand, the effect of CAII decreases quickly as pH_o increases. For high values of pH_o the extracellular binding and release of protons becomes the dominating bottleneck and the CAII reinforcement on the corresponding intracellular reactions makes little or no difference. An interesting property of Eq. 22 can be seen by putting either $[Lac^-_{in}]$ or $[Lac^-_{ex}]$ to zero. In both cases the dependence of the remaining lactate concentration vanishes. According to the model, the dependence of influx rate on lactate concentration is therefore only a consequence of a developing counter-transport.

In Eq. 21, the effect of CAII was included in the model as an increase of k_{12} and k_{21} with the common factor g_{CA}. This was motivated by assuming that proton exchange with the cytosol bulk was made more efficient by CAII. We will now elaborate on this idea. To start with, an observation from Fig. 5 gives an important hint of how the CAII-mechanism works. By adjusting the lactate concentration, fluxes of similar magnitude can be obtained for different extracellular pH. The flux rate at 10 mM lactate, pH_o 7.5 is of the same size as the flux rate at 0.3 mM, pH_o 6.0. However, the effect of CAII appears only to depend on the extracellular pH, not on the lactate concentration or the magnitude of the flux. The distribution of MCT1 proteins over the six states M_1-M_6 is the only way of accessing information about extracellular substrate concentrations at the inner side of the membrane. Therefore, two extracellular conditions yielding the same flux cannot be distinguished by any hypothetical CAII-mechanism that is not linked to the reactions included in kinetic model. In terms of the model, MCT1-CAII interaction is then restricted to alterations in the parameters of Eq. 22. Actually, since there is an evident effect of CAII in the efflux experiments (where $[Lac^-_{ex}]$ is zero), parameter alteration must include k_{12}, k_{56}, k_{65} or K_e. Changes in k_{56} and k_{65} are not very intuitive because of the intracellular location of CAII, but could not be dismissed with absolute certainty. Moreover, any changes must be done so that Eq. 20 is not violated. Decreasing K_e, coupled with an appropriate change in (at least) one other parameter, could enhance zero-*trans* efflux but the fit to the data obtained in the measurements is worse and for the influx experiment such changes give clearly erroneous results. These findings point to a change in k_{12} as the most likely effect of CAII on MCT1 within the model. Again, at least one more parameter must also be altered for Eq. 20 to hold. An equally sized increase in k_{21} is the only coupled alteration that gives the desired effect also for the influx experiments. A mutual increase of k_{12} and k_{21} with the factor g_{CA} preserves the equilibrium of the reaction between M_1 and M_2, and gives CAII an enhancing effect on transport activity, without shifting the equilibrium. As shown in former studies (21)(Becker & Deitmer, unpublished), the CAII induced enhancement of transport is not dependent on the enzymes catalytic activity, speeding up the interconversion of CO_2 and HCO_3^-, meaning that the enhancement is not due

to a faster equilibration with the CO_2 buffer system. Thus, the increase of the intracellular rate constants for binding and release of protons in the model must have a different physical interpretation. We hypothesize that by binding to MCT1, CAII provides additional binding sites for protons. Protonatable residues that are up to 12 Å apart from each other, could form proton-attractive domains, and could share the proton among them at a very fast rate, exceeding the upper limit of diffusion-controlled reactions (42). Negatively charged residues of membrane proteins with overlapping Coulomb cages can form a "proton-collecting antenna" that collects protons from solution and "funnels" them to the entrance of a proton-transfer pathway, or *vice versa*, can remove H^+ from the side of a transporter and pass them to the bulk solution (43, 44). By a collectively operating network of proton binding sites, established by CAII, the protonation and deprotonation rate of the MCT1 proton site could be accelerated, increasing the overall rate of transport.

A question about the CAII enhanced flux rate that needs to be addressed, given the proposed antenna effect, is whether it relies on binding of a single CAII molecule to an MCT1 or on some other principle. In the first scenario, CAII moves around in the vicinity of the membrane surface binding to MCT1 reversible. The fraction of MCT1-CAII complexes would then be dependent on the concentrations of both MCT1 and CAII. A more realistic model would instead of Eq. 22 be a linear combination of Eq. 15 and Eq. 22, $fT_{CA} + (1 - f)T$, where $f \in [0, 1]$ is the fraction of CAII-bound transporters. However, this model works worse due to the following reason. Comparing the effect of 50 and 200 ng CAII on transport activity during efflux of lactate reveals, that the enhancing effect is somewhere around half-saturated at 200 ng. This would mean that approximately 15% of the MCT1 are bound to a CAII at 50 ng. Since the other 85% would operate in the non-enhancing mode, the small fraction of MCT1-CAII would have to cope with the overall transport enhancement on their own. Such a high enhancement of only a small fraction of the MCT1 proteins is not compatible with Eq. 22, as it saturates for high values of g_{CA} before reaching the amplification needed. Another imaginable scenario is that the combination reaction of the two proteins is saturated already at an injection of 50 ng of CAII, resulting in a protein population more or less made up of MCT1-CAII complexes alone. A suggestion for how the enhancement mechanism still could be dependent on the CAII concentration would be that the CAII molecules themselves can bind, forming clusters or chains. Higher concentrations of CAII would mean larger CAII-structures connected to each MCT1, which in turn also could mean more effective antennas. In this scenario each MCT1 contributes a little to the overall enhancement, something that works better in the model compared to the two by two-case where a few MCT1 give a large contribution.

A simple model of the intracellular environment makes analysis of the MCT1 transport easier. Because of this, we have chosen to describe the concentrations of substrates and buffers as spatially homogenous although we know that this is an approximation. We use an "effective volume", smaller then the real cell volume, as an approximation of what happens in the vicinity of the electrode. For a more exact and realistic description of the intracellular species it would be necessary to employ a diffusion-reaction system governed by partial differential equations. Without a more detailed model it is hard to draw precise conclusions about exact parameter values. However, the homogenous approximation is a simplification that seems sufficient to explain the basic principles of MCT1 transport.

Acknowledgements

This research is funded by the Dependable Adaptive Systems and Mathematical Modeling (DASMOD) cluster of excellence, the Deutsche Forschungsgemeinschaft (De 231/16-4), the Swedish Foundation for Strategic Research, and the Gothenburg Mathematical Modeling Centre, which are all gratefully acknowledged.

References

[1] Halestrap, A. P., and D. Meredith, 2004. The SLC16 gene family - from monocarboxylate transporters (MCTs) to aromatic amino transporters and beyond. *Pflugers Arch* 447:619–628.

[2] Bergersen, L., 2007. Is lactate food for neurons? Comparison of monocarboxylate transporter subtypes in brain and muscle. *Neuroscience* 145:11–19.

[3] Schurr, A., C. West, and B. Rigor, 1988. Lactate-supported synaptic function in the rat hippocampal slice preparation. *Science* 240:1326–1328.

[4] Magistretti, P., L. Pellerin, D. Rothman, and R. Shulman, 1999. Energy on demand. *Science* 283:496–497.

[5] Pellerin, L., G. Pellegri, P. Bittar, Y. Charnay, C. Bouras, J. Martin, N. Stella, and P. Magistretti, 1998. Evidence supporting the existence of an activity-dependent astrocyte-neuron lactate shuttle. *Dev Neurosci* 20:291–299.

[6] Bouzier-Sore, A., S. Serres, P. Canioni, and M. Merle, 2003. Lactate involvement in neuron-glia metabolic interaction: (13)C-NMR spectroscopy contribution. *Biochimie* 85:841–848.

[7] Debernardi, R., K. Pierre, S. Lengacher, P. Magistretti, and L. Pellerin, 2003. Cell-specific expression pattern of monocarboxylate transporters in astrocytes and neurons observed in different mouse brain cortical cell cultures. *J Neurosci Res* 73:141–155.

[8] Hashimoto, T., S. Masuda, S. Taguchi, and G. Brooks, 2005. Immunohistochemical analysis of MCT1, MCT2 and MCT4 expression in rat plantaris muscle. *J Physiol* 567:121–129.

[9] Wilson, M., V. Jackson, C. Heddle, N. Price, H. Pilegaard, C. Juel, A. Bonen, I. Montgomery, O. Hutter, and A. Halestrap, 1998. Lactic acid efflux from white skeletal muscle is catalyzed by the monocarboxylate transporter isoform MCT3. *J Biol Chem* 273:15920–15926.

[10] Juel, C., 2001. Current aspects of lactate exchange: lactate/H^+ transport in human skeletal muscle. *Eur J Appl Physiol* 86:12–16.

[11] Brooks, G., 1998. Mammalian fuel utilization during sustained exercise. *Comp Biochem Physiol B Biochem Mol Biol* 120:89–107.

[12] Thomas, C., D. Bishop, T. Moore-Morris, and J. Mercier, 2007. Effects of high-intensity training on MCT1, MCT4, and NBC expressions in rat skeletal muscles: influence of chronic metabolic alkalosis. *Am J Physiol Endocrinol Metab* 293:E916–22.

[13] Bangsbo, J., C. Juel, Y. Hellsten, and B. Saltin, 1997. Dissociation between lactate and proton exchange in muscle during intense exercise in man. *J Physiol* 504:489–499.

[14] Juel, C., L. Grunnet, M. Holse, S. Kenworthy, V. Sommer, and T. Wulff, 2001. Reversibility of exercise-induced translocation of Na^+-K^+ pump subunits to the plasma membrane in rat skeletal muscle. *Pflugers Arch* 443:212–217.

[15] Poole, R., C. Sansom, and A. Halestrap, 1996. Studies of the membrane topology of the rat erythrocyte H^+/lactate cotransporter (MCT1). *Biochem J* 320:817–824.

[16] Bröer, S., H. Schneider, A. Bröer, B. Rahman, B. Hamprecht, and J. Deitmer, 1998. Characterization of the monocarboxylate transporter 1 expressed in *Xenopus laevis* oocytes by changes in cytosolic pH. *Biochem J* 333:167–174.

[17] de Bruijne, A., H. Vreeburg, and J. van Stevenick, 1983. Kinetic analysis of L-lactate transport in human erythrocytes via the monocarboxylate-specific carrier system. *Biochim Biophys Acta* 732:562–568.

[18] Juel, C., and A. Halestrap, 1999. Lactate transport in skeletal muscle - role and regulation of the monocarboxylate transporter. *J Physiol* 517:633–642.

[19] Galic, S., H.-P. Schneider, A. Bröer, J. W. Deitmer, and S. Bröer, 2003. The loop between helix 4 and helix 5 in the monocarboxylate transporter MCT1 is important for substrate selection and protein stability. *Biochem J* 376:413–422.

[20] Becker, H., S. Broer, and J. Deitmer, 2004. Facilitated lactate transport by MCT1 when coexpressed with the sodium bicarbonate cotransporter (NBC) in *Xenopus* oocytes. *Biophys J* 86:235–247.

[21] Becker, H. M., C. Fecher-Trost, D. Hirnet, D. Sültemeyer, and J. W. Deitmer, 2005. transport activity of MCT1 expressed in *Xenopus* oocytes is increased by interaction with carbonic anhydrase. *J Biol Chem* .

[22] Becker, H. M., and J. W. Deitmer, 2007. Carbonic anhydrase II increases the activity of the human electrogenic Na^+/HCO_3^- cotransporter. *J Biol Chem* 282:13508–13521.

[23] Pushkin, A., N. Abuladze, E. Gross, D. Newman, S. Tatishchev, I. Lee, O. Fedotoff, G. Bondar, R. Azimov, M. Ngyuen, and I. Kurtz, 2004. Molecular mechanism of kNBC1-carbonic anhydrase II interaction in proximal tubule cells. *J Physiol* 559:55–65.

[24] Vince, J. W., and R. A. Reithmeier, 1998. Carbonic anhydrase II binds to the carboxyl terminus of human band 3, the erythrocyte Cl^+/HCO_3^- exchanger. *J Biol Chem* 273:28430–28437.

[25] Li, X., B. Alvarez, J. R. Casey, R. A. Reithmeier, and L. Fliegel, 2002. Carbonic anhydrase II binds to and enhances activity of the Na^+/H^+ exchanger. *J Biol Chem* 277:36085–36091.

[26] Juel, C., C. Lundby, M. Sander, J. Calbet, and G. van Hall, 2003. Human skeletal muscle and erythrocyte proteins involved in acid-base homeostasis: adaptations to chronic hypoxia. *J Physiol* 548:639–648.

[27] Wetzel, P., A. Hasse, S. Papadopoulos, J. Voipio, K. Kaila, and G. Gros, 2001. Extracellular carbonic anhydrase activity facilitates lactic acid transport in rat skeletal muscle fibres. *J Physiol* 531:743–756.

[28] Deitmer, J., and C. Rose, 1996. pH regulation and proton signalling by glial cells. *Prog Neurobiol* 48:73–103.

[29] Svichar, N., and M. Chesler, 2003. Surface carbonic anhydrase activity on astrocytes and neurons facilitates lactate transport. *Glia* 41:415–419.

[30] Fall, C., E. Marland, J. Wagner, and J. Tyson, 2002. Computational cell biology. Springer-Verlag.

[31] Klipp, E., R. Herwig, A. Kowald, C. Wierling, and H. Lehrach, 2005. Systems biology in practice. Wiley-VCH.

[32] Szallasi, Z., J. Stelling, and V. Periwal, 2006. System modeling in cellular biology. MIT Press.

[33] Bower, J., and H. Bolouri, 2001. Computational modeling of genetic and biochemical networks. MIT Press.

[34] Bröer, S., B. Rahman, G. Pellegri, L. Pellerin, J. Martin, S. Verleysdonk, B. Hamprecht, and P. Magistretti, 1997. Comparison of lactate transport in astroglial cells and monocarboxylate transporter 1 (MCT1) expressing *Xenopus laevis* oocytes. Expression of two different monocarboxylate transporters in astroglial cells and neurons. *J Biol Chem* 272:30096–30102.

[35] Deitmer, J., 1991. Electrogenic sodium-dependent bicarbonate secretion by glial cells of the leech central nervous system. *J Gen Physiol* 98:637–655.

[36] Schimdt, H., 2005. SBTOOLBOX: Systems Biology Toolbox for MATLAB. http://www.sbtoolbox.org.

[37] Schimdt, H., 2006. SBADDON: High performance simulation interface and parameter estimation framework for MATLAB. http://www.sbtoolbox.org/SBaddon.

[38] Ädelroth, P., and P. Brzezinski, 2004. Surface-mediated proton-transfer reactions in membrane-bound proteins. *Biochim Biophys Acta* 1655:102–115.

[39] Deuticke, B., 1982. Monocarboxylate transport in erythrocytes. *J. Membrane Biol.* 70:89–103.

[40] Lytle, C., T. McManus, and M. Haas, 1998. A model of Na-K-2Cl cotransport based on ordered ion binding and glide symmetry. *Am J Physiol Cell Physiol* 274:299–309.

[41] Hopfer, U., and R. Groseclose, 1980. The mechanism of Na^+-dependent D-Glucose transport. *J Biol Chem* 255:4453–4462.

[42] Gutman, M., E. Nachliel, and R. Friedman, 2006. The dynamics of proton transfer between adjacent sites. *Photochem. Photobiol. Sci.* 5:531–537.

[43] Brändén, M., T. Sandén, P. Brzezinski, and J. Widengren, 2006. Localized proton microcircuits at the biological membranewater interface. *PNAS* 103:19766–19770.

[44] Georgievskii, Y., E. Medvedev, and A. Stuchebrukhov, 2002. Proton Transport via the Membrane Surface. *Biophys J* 82:2833–2846.

Published reports of the Fraunhofer ITWM

The PDF-files of the following reports are available under:
www.itwm.fraunhofer.de/de/zentral__berichte/berichte

1. D. Hietel, K. Steiner, J. Struckmeier
A Finite - Volume Particle Method for Compressible Flows
(19 pages, 1998)

2. M. Feldmann, S. Seibold
Damage Diagnosis of Rotors: Application of Hilbert Transform and Multi-Hypothesis Testing
Keywords: Hilbert transform, damage diagnosis, Kalman filtering, non-linear dynamics
(23 pages, 1998)

3. Y. Ben-Haim, S. Seibold
Robust Reliability of Diagnostic Multi-Hypothesis Algorithms: Application to Rotating Machinery
Keywords: Robust reliability, convex models, Kalman filtering, multi-hypothesis diagnosis, rotating machinery, crack diagnosis
(24 pages, 1998)

4. F.-Th. Lentes, N. Siedow
Three-dimensional Radiative Heat Transfer in Glass Cooling Processes
(23 pages, 1998)

5. A. Klar, R. Wegener
A hierarchy of models for multilane vehicular traffic
Part I: Modeling
(23 pages, 1998)

Part II: Numerical and stochastic investigations
(17 pages, 1998)

6. A. Klar, N. Siedow
Boundary Layers and Domain Decomposition for Radiative Heat Transfer and Diffusion Equations: Applications to Glass Manufacturing Processes
(24 pages, 1998)

7. I. Choquet
Heterogeneous catalysis modelling and numerical simulation in rarified gas flows Part I: Coverage locally at equilibrium
(24 pages, 1998)

8. J. Ohser, B. Steinbach, C. Lang
Efficient Texture Analysis of Binary Images
(17 pages, 1998)

9. J. Orlik
Homogenization for viscoelasticity of the integral type with aging and shrinkage
(20 pages, 1998)

10. J. Mohring
Helmholtz Resonators with Large Aperture
(21 pages, 1998)

11. H. W. Hamacher, A. Schöbel
On Center Cycles in Grid Graphs
(15 pages, 1998)

12. H. W. Hamacher, K.-H. Küfer
Inverse radiation therapy planning - a multiple objective optimisation approach
(14 pages, 1999)

13. C. Lang, J. Ohser, R. Hilfer
On the Analysis of Spatial Binary Images
(20 pages, 1999)

14. M. Junk
On the Construction of Discrete Equilibrium Distributions for Kinetic Schemes
(24 pages, 1999)

15. M. Junk, S. V. Raghurame Rao
A new discrete velocity method for Navier-Stokes equations
(20 pages, 1999)

16. H. Neunzert
Mathematics as a Key to Key Technologies
(39 pages (4 PDF-Files), 1999)

17. J. Ohser, K. Sandau
Considerations about the Estimation of the Size Distribution in Wicksell's Corpuscle Problem
(18 pages, 1999)

18. E. Carrizosa, H. W. Hamacher, R. Klein, S. Nickel
Solving nonconvex planar location problems by finite dominating sets
Keywords: Continuous Location, Polyhedral Gauges, Finite Dominating Sets, Approximation, Sandwich Algorithm, Greedy Algorithm
(19 pages, 2000)

19. A. Becker
A Review on Image Distortion Measures
Keywords: Distortion measure, human visual system
(26 pages, 2000)

20. H. W. Hamacher, M. Labbé, S. Nickel, T. Sonneborn
Polyhedral Properties of the Uncapacitated Multiple Allocation Hub Location Problem
Keywords: integer programming, hub location, facility location, valid inequalities, facets, branch and cut
(21 pages, 2000)

21. H. W. Hamacher, A. Schöbel
Design of Zone Tariff Systems in Public Transportation
(30 pages, 2001)

22. D. Hietel, M. Junk, R. Keck, D. Teleaga
The Finite-Volume-Particle Method for Conservation Laws
(16 pages, 2001)

23. T. Bender, H. Hennes, J. Kalcsics, M. T. Melo, S. Nickel
Location Software and Interface with GIS and Supply Chain Management
Keywords: facility location, software development, geographical information systems, supply chain management
(48 pages, 2001)

24. H. W. Hamacher, S. A. Tjandra
Mathematical Modelling of Evacuation Problems: A State of Art
(44 pages, 2001)

25. J. Kuhnert, S. Tiwari
Grid free method for solving the Poisson equation
Keywords: Poisson equation, Least squares method, Grid free method
(19 pages, 2001)

26. T. Götz, H. Rave, D. Reinel-Bitzer, K. Steiner, H. Tiemeier
Simulation of the fiber spinning process
Keywords: Melt spinning, fiber model, Lattice Boltzmann, CFD
(19 pages, 2001)

27. A. Zemitis
On interaction of a liquid film with an obstacle
Keywords: impinging jets, liquid film, models, numerical solution, shape
(22 pages, 2001)

28. I. Ginzburg, K. Steiner
Free surface lattice-Boltzmann method to model the filling of expanding cavities by Bingham Fluids
Keywords: Generalized LBE, free-surface phenomena, interface boundary conditions, filling processes, Bingham viscoplastic model, regularized models
(22 pages, 2001)

29. H. Neunzert
»Denn nichts ist für den Menschen als Menschen etwas wert, was er nicht mit Leidenschaft tun kann«
Vortrag anlässlich der Verleihung des Akademiepreises des Landes Rheinland-Pfalz am 21.11.2001
Keywords: Lehre, Forschung, angewandte Mathematik, Mehrskalenanalyse, Strömungsmechanik
(18 pages, 2001)

30. J. Kuhnert, S. Tiwari
Finite pointset method based on the projection method for simulations of the incompressible Navier-Stokes equations
Keywords: Incompressible Navier-Stokes equations, Meshfree method, Projection method, Particle scheme, Least squares approximation
AMS subject classification: 76D05, 76M28
(25 pages, 2001)

31. R. Korn, M. Krekel
Optimal Portfolios with Fixed Consumption or Income Streams
Keywords: Portfolio optimisation, stochastic control, HJB equation, discretisation of control problems
(23 pages, 2002)

32. M. Krekel
Optimal portfolios with a loan dependent credit spread
Keywords: Portfolio optimisation, stochastic control, HJB equation, credit spread, log utility, power utility, non-linear wealth dynamics
(25 pages, 2002)

33. J. Ohser, W. Nagel, K. Schladitz
The Euler number of discretized sets – on the choice of adjacency in homogeneous lattices
Keywords: image analysis, Euler number, neighborhod relationships, cuboidal lattice
(32 pages, 2002)

34. I. Ginzburg, K. Steiner
Lattice Boltzmann Model for Free-Surface flow and Its Application to Filling Process in Casting
Keywords: Lattice Boltzmann models; free-surface phenomena; interface boundary conditions; filling processes; injection molding; volume of fluid method; interface boundary conditions; advection-schemes; upwind-schemes
(54 pages, 2002)

35. M. Günther, A. Klar, T. Materne, R. Wegener
Multivalued fundamental diagrams and stop and go waves for continuum traffic equations
Keywords: traffic flow, macroscopic equations, kinetic derivation, multivalued fundamental diagram, stop and go waves, phase transitions
(25 pages, 2002)

36. S. Feldmann, P. Lang, D. Prätzel-Wolters
Parameter influence on the zeros of network determinants
Keywords: Networks, Equicofactor matrix polynomials, Realization theory, Matrix perturbation theory
(30 pages, 2002)

37. K. Koch, J. Ohser, K. Schladitz
Spectral theory for random closed sets and estimating the covariance via frequency space
Keywords: Random set, Bartlett spectrum, fast Fourier transform, power spectrum
(28 pages, 2002)

38. D. d'Humières, I. Ginzburg
Multi-reflection boundary conditions for lattice Boltzmann models
Keywords: lattice Boltzmann equation, boudary condistions, bounce-back rule, Navier-Stokes equation
(72 pages, 2002)

39. R. Korn
Elementare Finanzmathematik
Keywords: Finanzmathematik, Aktien, Optionen, Portfolio-Optimierung, Börse, Lehrerweiterbildung, Mathematikunterricht
(98 pages, 2002)

40. J. Kallrath, M. C. Müller, S. Nickel
Batch Presorting Problems: Models and Complexity Results
Keywords: Complexity theory, Integer programming, Assigment, Logistics
(19 pages, 2002)

41. J. Linn
On the frame-invariant description of the phase space of the Folgar-Tucker equation
Key words: fiber orientation, Folgar-Tucker equation, injection molding
(5 pages, 2003)

42. T. Hanne, S. Nickel
A Multi-Objective Evolutionary Algorithm for Scheduling and Inspection Planning in Software Development Projects
Key words: multiple objective programming, project management and scheduling, software development, evolutionary algorithms, efficient set
(29 pages, 2003)

43. T. Bortfeld , K.-H. Küfer, M. Monz, A. Scherrer, C. Thieke, H. Trinkaus
Intensity-Modulated Radiotherapy - A Large Scale Multi-Criteria Programming Problem
Keywords: multiple criteria optimization, representative systems of Pareto solutions, adaptive triangulation, clustering and disaggregation techniques, visualization of Pareto solutions, medical physics, external beam radiotherapy planning, intensity modulated radiotherapy
(31 pages, 2003)

44. T. Halfmann, T. Wichmann
Overview of Symbolic Methods in Industrial Analog Circuit Design
Keywords: CAD, automated analog circuit design, symbolic analysis, computer algebra, behavioral modeling, system simulation, circuit sizing, macro modeling, differential-algebraic equations, index
(17 pages, 2003)

45. S. E. Mikhailov, J. Orlik
Asymptotic Homogenisation in Strength and Fatigue Durability Analysis of Composites
Keywords: multiscale structures, asymptotic homogenization, strength, fatigue, singularity, non-local conditions
(14 pages, 2003)

46. P. Domínguez-Marín, P. Hansen, N. Mladenovi´c , S. Nickel
Heuristic Procedures for Solving the Discrete Ordered Median Problem
Keywords: genetic algorithms, variable neighborhood search, discrete facility location
(31 pages, 2003)

47. N. Boland, P. Domínguez-Marín, S. Nickel, J. Puerto
Exact Procedures for Solving the Discrete Ordered Median Problem
Keywords: discrete location, Integer programming
(41 pages, 2003)

48. S. Feldmann, P. Lang
Padé-like reduction of stable discrete linear systems preserving their stability
Keywords: Discrete linear systems, model reduction, stability, Hankel matrix, Stein equation
(16 pages, 2003)

49. J. Kallrath, S. Nickel
A Polynomial Case of the Batch Presorting Problem
Keywords: batch presorting problem, online optimization, competetive analysis, polynomial algorithms, logistics
(17 pages, 2003)

50. T. Hanne, H. L. Trinkaus
knowCube for MCDM – Visual and Interactive Support for Multicriteria Decision Making
Key words: Multicriteria decision making, knowledge management, decision support systems, visual interfaces, interactive navigation, real-life applications.
(26 pages, 2003)

51. O. Iliev, V. Laptev
On Numerical Simulation of Flow Through Oil Filters
Keywords: oil filters, coupled flow in plain and porous media, Navier-Stokes, Brinkman, numerical simulation
(8 pages, 2003)

52. W. Dörfler, O. Iliev, D. Stoyanov, D. Vassileva
On a Multigrid Adaptive Refinement Solver for Saturated Non-Newtonian Flow in Porous Media
Keywords: Nonlinear multigrid, adaptive refinement, non-Newtonian flow in porous media
(17 pages, 2003)

53. S. Kruse
On the Pricing of Forward Starting Options under Stochastic Volatility
Keywords: Option pricing, forward starting options, Heston model, stochastic volatility, cliquet options
(11 pages, 2003)

54. O. Iliev, D. Stoyanov
Multigrid – adaptive local refinement solver for incompressible flows
Keywords: Navier-Stokes equations, incompressible flow, projection-type splitting, SIMPLE, multigrid methods, adaptive local refinement, lid-driven flow in a cavity
(37 pages, 2003)

55. V. Starikovicius
The multiphase flow and heat transfer in porous media
Keywords: Two-phase flow in porous media, various formulations, global pressure, multiphase mixture model, numerical simulation
(30 pages, 2003)

56. P. Lang, A. Sarishvili, A. Wirsen
Blocked neural networks for knowledge extraction in the software development process
Keywords: Blocked Neural Networks, Nonlinear Regression, Knowledge Extraction, Code Inspection
(21 pages, 2003)

57. H. Knaf, P. Lang, S. Zeiser
Diagnosis aiding in Regulation Thermography using Fuzzy Logic
Keywords: fuzzy logic,knowledge representation, expert system
(22 pages, 2003)

58. M. T. Melo, S. Nickel, F. Saldanha da Gama
Largescale models for dynamic multicommodity capacitated facility location
Keywords: supply chain management, strategic planning, dynamic location, modeling
(40 pages, 2003)

59. J. Orlik
Homogenization for contact problems with periodically rough surfaces
Keywords: asymptotic homogenization, contact problems
(28 pages, 2004)

60. A. Scherrer, K.-H. Küfer, M. Monz, F. Alonso, T. Bortfeld
IMRT planning on adaptive volume structures – a significant advance of computational complexity
Keywords: Intensity-modulated radiation therapy (IMRT), inverse treatment planning, adaptive volume structures, hierarchical clustering, local refinement, adaptive clustering, convex programming, mesh generation, multi-grid methods
(24 pages, 2004)

61. D. Kehrwald
Parallel lattice Boltzmann simulation of complex flows
Keywords: Lattice Boltzmann methods, parallel computing, microstructure simulation, virtual material design, pseudo-plastic fluids, liquid composite moulding
(12 pages, 2004)

62. O. Iliev, J. Linn, M. Moog, D. Niedziela, V. Starikovicius
On the Performance of Certain Iterative Solvers for Coupled Systems Arising in Discretization of Non-Newtonian Flow Equations
Keywords: Performance of iterative solvers, Preconditioners, Non-Newtonian flow
(17 pages, 2004)

63. R. Ciegis, O. Iliev, S. Rief, K. Steiner
On Modelling and Simulation of Different Regimes for Liquid Polymer Moulding
Keywords: Liquid Polymer Moulding, Modelling, Simulation, Infiltration, Front Propagation, non-Newtonian flow in porous media
(43 pages, 2004)

64. T. Hanne, H. Neu
Simulating Human Resources in Software Development Processes
Keywords: Human resource modeling, software process, productivity, human factors, learning curve
(14 pages, 2004)

65. O. Iliev, A. Mikelic, P. Popov
Fluid structure interaction problems in deformable porous media: Toward permeability of deformable porous media
Keywords: fluid-structure interaction, deformable porous media, upscaling, linear elasticity, stokes, finite elements
(28 pages, 2004)

66. F. Gaspar, O. Iliev, F. Lisbona, A. Naumovich, P. Vabishchevich
On numerical solution of 1-D poroelasticity equations in a multilayered domain
Keywords: poroelasticity, multilayered material, finite volume discretization, MAC type grid
(41 pages, 2004)

67. J. Ohser, K. Schladitz, K. Koch, M. Nöthe
Diffraction by image processing and its application in materials science
Keywords: porous microstructure, image analysis, random set, fast Fourier transform, power spectrum, Bartlett spectrum
(13 pages, 2004)

68. H. Neunzert
Mathematics as a Technology: Challenges for the next 10 Years
Keywords: applied mathematics, technology, modelling, simulation, visualization, optimization, glass processing, spinning processes, fiber-fluid interaction, trubulence effects, topological optimization, multicriteria optimization, Uncertainty and Risk, financial mathematics, Malliavin calculus, Monte-Carlo methods, virtual material design, filtration, bio-informatics, system biology
(29 pages, 2004)

69. R. Ewing, O. Iliev, R. Lazarov, A. Naumovich
On convergence of certain finite difference discretizations for 1D poroelasticity interface problems
Keywords: poroelasticity, multilayered material, finite volume discretizations, MAC type grid, error estimates
(26 pages,2004)

70. W. Dörfler, O. Iliev, D. Stoyanov, D. Vassileva
On Efficient Simulation of Non-Newtonian Flow in Saturated Porous Media with a Multigrid Adaptive Refinement Solver
Keywords: Nonlinear multigrid, adaptive renement, non-Newtonian in porous media
(25 pages, 2004)

71. J. Kalcsics, S. Nickel, M. Schröder
Towards a Unified Territory Design Approach – Applications, Algorithms and GIS Integration
Keywords: territory desgin, political districting, sales territory alignment, optimization algorithms, Geographical Information Systems
(40 pages, 2005)

72. K. Schladitz, S. Peters, D. Reinel-Bitzer, A. Wiegmann, J. Ohser
Design of acoustic trim based on geometric modeling and flow simulation for non-woven
Keywords: random system of fibers, Poisson line process, flow resistivity, acoustic absorption, Lattice-Boltzmann method, non-woven
(21 pages, 2005)

73. V. Rutka, A. Wiegmann
Explicit Jump Immersed Interface Method for virtual material design of the effective elastic moduli of composite materials
Keywords: virtual material design, explicit jump immersed interface method, effective elastic moduli, composite materials
(22 pages, 2005)

74. T. Hanne
Eine Übersicht zum Scheduling von Baustellen
Keywords: Projektplanung, Scheduling, Bauplanung, Bauindustrie
(32 pages, 2005)

75. J. Linn
The Folgar-Tucker Model as a Differetial Algebraic System for Fiber Orientation Calculation
Keywords: fiber orientation, Folgar–Tucker model, invariants, algebraic constraints, phase space, trace stability
(15 pages, 2005)

76. M. Speckert, K. Dreßler, H. Mauch, A. Lion, G. J. Wierda
Simulation eines neuartigen Prüfsystems für Achserprobungen durch MKS-Modellierung einschließlich Regelung
Keywords: virtual test rig, suspension testing, multibody simulation, modeling hexapod test rig, optimization of test rig configuration
(20 pages, 2005)

77. K.-H. Küfer, M. Monz, A. Scherrer, P. Süss, F. Alonso, A. S. A. Sultan, Th. Bortfeld, D. Craft, Chr. Thieke
Multicriteria optimization in intensity modulated radiotherapy planning
Keywords: multicriteria optimization, extreme solutions, real-time decision making, adaptive approximation schemes, clustering methods, IMRT planning, reverse engineering
(51 pages, 2005)

78. S. Amstutz, H. Andrä
A new algorithm for topology optimization using a level-set method
Keywords: shape optimization, topology optimization, topological sensitivity, level-set
(22 pages, 2005)

79. N. Ettrich
Generation of surface elevation models for urban drainage simulation
Keywords: Flooding, simulation, urban elevation models, laser scanning
(22 pages, 2005)

80. H. Andrä, J. Linn, I. Matei, I. Shklyar, K. Steiner, E. Teichmann
OPTCAST – Entwicklung adäquater Strukturoptimierungsverfahren für Gießereien Technischer Bericht (KURZFASSUNG)
Keywords: Topologieoptimierung, Level-Set-Methode, Gießprozesssimulation, Gießtechnische Restriktionen, CAE-Kette zur Strukturoptimierung
(77 pages, 2005)

81. N. Marheineke, R. Wegener
Fiber Dynamics in Turbulent Flows Part I: General Modeling Framework
Keywords: fiber-fluid interaction; Cosserat rod; turbulence modeling; Kolmogorov's energy spectrum; double-velocity correlations; differentiable Gaussian fields
(20 pages, 2005)

Part II: Specific Taylor Drag
Keywords: flexible fibers; k-ε turbulence model; fiber-turbulence interaction scales; air drag; random Gaussian aerodynamic force; white noise; stochastic differential equations; ARMA process
(18 pages, 2005)

82. C. H. Lampert, O. Wirjadi
An Optimal Non-Orthogonal Separation of the Anisotropic Gaussian Convolution Filter
Keywords: Anisotropic Gaussian filter, linear filtering, orientation space, nD image processing, separable filters
(25 pages, 2005)

83. H. Andrä, D. Stoyanov
Error indicators in the parallel finite element solver for linear elasticity DDFEM
Keywords: linear elasticity, finite element method, hierarchical shape functions, domain decom-position, parallel implementation, a posteriori error estimates
(21 pages, 2006)

84. M. Schröder, I. Solchenbach
Optimization of Transfer Quality in Regional Public Transit
Keywords: public transit, transfer quality, quadratic assignment problem
(16 pages, 2006)

85. A. Naumovich, F. J. Gaspar
On a multigrid solver for the three-dimensional Biot poroelasticity system in multilayered domains
Keywords: poroelasticity, interface problem, multigrid, operator-dependent prolongation
(11 pages, 2006)

86. S. Panda, R. Wegener, N. Marheineke
Slender Body Theory for the Dynamics of Curved Viscous Fibers
Keywords: curved viscous fibers; fluid dynamics; Navier-Stokes equations; free boundary value problem; asymptotic expansions; slender body theory
(14 pages, 2006)

87. E. Ivanov, H. Andrä, A. Kudryavtsev
Domain Decomposition Approach for Automatic Parallel Generation of Tetrahedral Grids
Key words: Grid Generation, Unstructured Grid, Delaunay Triangulation, Parallel Programming, Domain Decomposition, Load Balancing
(18 pages, 2006)

88. S. Tiwari, S. Antonov, D. Hietel, J. Kuhnert, R. Wegener
A Meshfree Method for Simulations of Interactions between Fluids and Flexible Structures
Key words: Meshfree Method, FPM, Fluid Structure Interaction, Sheet of Paper, Dynamical Coupling
(16 pages, 2006)

89. R. Ciegis , O. Iliev, V. Starikovicius, K. Steiner
Numerical Algorithms for Solving Problems of Multiphase Flows in Porous Media
Keywords: nonlinear algorithms, finite-volume method, software tools, porous media, flows
(16 pages, 2006)

90. D. Niedziela, O. Iliev, A. Latz
On 3D Numerical Simulations of Viscoelastic Fluids
Keywords: non-Newtonian fluids, anisotropic viscosity, integral constitutive equation
(18 pages, 2006)

91. A. Winterfeld
Application of general semi-infinite Programming to Lapidary Cutting Problems
Keywords: large scale optimization, nonlinear programming, general semi-infinite optimization, design centering, clustering
(26 pages, 2006)

92. J. Orlik, A. Ostrovska
Space-Time Finite Element Approximation and Numerical Solution of Hereditary Linear Viscoelasticity Problems
Keywords: hereditary viscoelasticity; kern approximation by interpolation; space-time finite element approximation, stability and a priori estimate
(24 pages, 2006)

93. V. Rutka, A. Wiegmann, H. Andrä
EJIIM for Calculation of effective Elastic Moduli in 3D Linear Elasticity
Keywords: Elliptic PDE, linear elasticity, irregular domain, finite differences, fast solvers, effective elastic moduli
(24 pages, 2006)

94. A. Wiegmann, A. Zemitis
EJ-HEAT: A Fast Explicit Jump Harmonic Averaging Solver for the Effective Heat Conductivity of Composite Materials
Keywords: Stationary heat equation, effective thermal conductivity, explicit jump, discontinuous coefficients, virtual material design, microstructure simulation, EJ-HEAT
(21 pages, 2006)

95. A. Naumovich
On a finite volume discretization of the three-dimensional Biot poroelasticity system in multilayered domains
Keywords: Biot poroelasticity system, interface problems, finite volume discretization, finite difference method
(21 pages, 2006)

96. M. Krekel, J. Wenzel
A unified approach to Credit Default Swaption and Constant Maturity Credit Default Swap valuation
Keywords: LIBOR market model, credit risk, Credit Default Swaption, Constant Maturity Credit Default Swap-method
(43 pages, 2006)

97. A. Dreyer
Interval Methods for Analog Circiuts
Keywords: interval arithmetic, analog circuits, tolerance analysis, parametric linear systems, frequency response, symbolic analysis, CAD, computer algebra
(36 pages, 2006)

98. N. Weigel, S. Weihe, G. Bitsch, K. Dreßler
Usage of Simulation for Design and Optimization of Testing
Keywords: Vehicle test rigs, MBS, control, hydraulics, testing philosophy
(14 pages, 2006)

99. H. Lang, G. Bitsch, K. Dreßler, M. Speckert
Comparison of the solutions of the elastic and elastoplastic boundary value problems
Keywords: Elastic BVP, elastoplastic BVP, variational inequalities, rate-independency, hysteresis, linear kinematic hardening, stop- and play-operator
(21 pages, 2006)

100. M. Speckert, K. Dreßler, H. Mauch
MBS Simulation of a hexapod based suspension test rig
Keywords: Test rig, MBS simulation, suspension, hydraulics, controlling, design optimization
(12 pages, 2006)

101. S. Azizi Sultan, K.-H. Küfer
A dynamic algorithm for beam orientations in multicriteria IMRT planning
Keywords: radiotherapy planning, beam orientation optimization, dynamic approach, evolutionary algorithm, global optimization
(14 pages, 2006)

102. T. Götz, A. Klar, N. Marheineke, R. Wegener
A Stochastic Model for the Fiber Lay-down Process in the Nonwoven Production
Keywords: fiber dynamics, stochastic Hamiltonian system, stochastic averaging
(17 pages, 2006)

103. Ph. Süss, K.-H. Küfer
Balancing control and simplicity: a variable aggregation method in intensity modulated radiation therapy planning
Keywords: IMRT planning, variable aggregation, clustering methods
(22 pages, 2006)

104. A. Beaudry, G. Laporte, T. Melo, S. Nickel
Dynamic transportation of patients in hospitals
Keywords: in-house hospital transportation, dial-a-ride, dynamic mode, tabu search
(37 pages, 2006)

105. Th. Hanne
Applying multiobjective evolutionary algorithms in industrial projects
Keywords: multiobjective evolutionary algorithms, discrete optimization, continuous optimization, electronic circuit design, semi-infinite programming, scheduling
(18 pages, 2006)

106. J. Franke, S. Halim
Wild bootstrap tests for comparing signals and images
Keywords: wild bootstrap test, texture classification, textile quality control, defect detection, kernel estimate, nonparametric regression
(13 pages, 2007)

107. Z. Drezner, S. Nickel
Solving the ordered one-median problem in the plane
Keywords: planar location, global optimization, ordered median, big triangle small triangle method, bounds, numerical experiments
(21 pages, 2007)

108. Th. Götz, A. Klar, A. Unterreiter, R. Wegener
Numerical evidance for the non-existing of solutions of the equations desribing rotational fiber spinning
Keywords: rotational fiber spinning, viscous fibers, boundary value problem, existence of solutions
(11 pages, 2007)

109. Ph. Süss, K.-H. Küfer
Smooth intensity maps and the Bortfeld-Boyer sequencer
Keywords: probabilistic analysis, intensity modulated radiotherapy treatment (IMRT), IMRT plan application, step-and-shoot sequencing
(8 pages, 2007)

110. E. Ivanov, O. Gluchshenko, H. Andrä, A. Kudryavtsev
Parallel software tool for decomposing and meshing of 3d structures
Keywords: a-priori domain decomposition, unstructured grid, Delaunay mesh generation
(14 pages, 2007)

111. O. Iliev, R. Lazarov, J. Willems
Numerical study of two-grid preconditioners for 1d elliptic problems with highly oscillating discontinuous coefficients
Keywords: two-grid algorithm, oscillating coefficients, preconditioner
(20 pages, 2007)

112. L. Bonilla, T. Götz, A. Klar, N. Marheineke, R. Wegener
Hydrodynamic limit of the Fokker-Planck-equation describing fiber lay-down processes
Keywords: stochastic dierential equations, Fokker-Planck equation, asymptotic expansion, Ornstein-Uhlenbeck process
(17 pages, 2007)

113. S. Rief
Modeling and simulation of the pressing section of a paper machine
Keywords: paper machine, computational fluid dynamics, porous media
(41 pages, 2007)

114. R. Ciegis, O. Iliev, Z. Lakdawala
On parallel numerical algorithms for simulating industrial filtration problems
Keywords: Navier-Stokes-Brinkmann equations, finite volume discretization method, SIMPLE, parallel computing, data decomposition method
(24 pages, 2007)

115. N. Marheineke, R. Wegener
Dynamics of curved viscous fibers with surface tension
Keywords: Slender body theory, curved viscous bers with surface tension, free boundary value problem
(25 pages, 2007)

116. S. Feth, J. Franke, M. Speckert
Resampling-Methoden zur mse-Korrektur und Anwendungen in der Betriebsfestigkeit
Keywords: Weibull, Bootstrap, Maximum-Likelihood, Betriebsfestigkeit
(16 pages, 2007)

117. H. Knaf
Kernel Fisher discriminant functions – a concise and rigorous introduction
Keywords: wild bootstrap test, texture classification, textile quality control, defect detection, kernel estimate, nonparametric regression
(30 pages, 2007)

118. O. Iliev, I. Rybak
On numerical upscaling for flows in heterogeneous porous media
Keywords: numerical upscaling, heterogeneous porous media, single phase flow, Darcy's law, multiscale problem, effective permeability, multipoint flux approximation, anisotropy
(17 pages, 2007)

119. O. Iliev, I. Rybak
On approximation property of multipoint flux approximation method
Keywords: Multipoint flux approximation, finite volume method, elliptic equation, discontinuous tensor coefficients, anisotropy
(15 pages, 2007)

120. O. Iliev, I. Rybak, J. Willems
On upscaling heat conductivity for a class of industrial problems
Keywords: Multiscale problems, effective heat conductivity, numerical upscaling, domain decomposition
(21 pages, 2007)

121. R. Ewing, O. Iliev, R. Lazarov, I. Rybak
On two-level preconditioners for flow in porous media
Keywords: Multiscale problem, Darcy's law, single phase flow, anisotropic heterogeneous porous media, numerical upscaling, multigrid, domain decomposition, efficient preconditioner
(18 pages, 2007)

122. M. Brickenstein, A. Dreyer
POLYBORI: A Gröbner basis framework for Boolean polynomials
Keywords: Gröbner basis, formal verification, Boolean polynomials, algebraic cryptoanalysis, satisfiability
(23 pages, 2007)

123. O. Wirjadi
Survey of 3d image segmentation methods
Keywords: image processing, 3d, image segmentation, binarization
(20 pages, 2007)

124. S. Zeytun, A. Gupta
A Comparative Study of the Vasicek and the CIR Model of the Short Rate
Keywords: interest rates, Vasicek model, CIR-model, calibration, parameter estimation
(17 pages, 2007)

125. G. Hanselmann, A. Sarishvili
Heterogeneous redundancy in software quality prediction using a hybrid Bayesian approach
Keywords: reliability prediction, fault prediction, non-homogeneous poisson process, Bayesian model averaging
(17 pages, 2007)

126. V. Maag, M. Berger, A. Winterfeld, K.-H. Küfer
A novel non-linear approach to minimal area rectangular packing
Keywords: rectangular packing, non-overlapping constraints, non-linear optimization, regularization, relaxation
(18 pages, 2007)

127. M. Monz, K.-H. Küfer, T. Bortfeld, C. Thieke
Pareto navigation – systematic multi-criteria-based IMRT treatment plan determination
Keywords: convex, interactive multi-objective optimization, intensity modulated radiotherapy planning
(15 pages, 2007)

128. M. Krause, A. Scherrer
On the role of modeling parameters in IMRT plan optimization
Keywords: intensity-modulated radiotherapy (IMRT), inverse IMRT planning, convex optimization, sensitivity analysis, elasticity, modeling parameters, equivalent uniform dose (EUD)
(18 pages, 2007)

129. A. Wiegmann
Computation of the permeability of porous materials from their microstructure by FFF-Stokes
Keywords: permeability, numerical homogenization, fast Stokes solver
(24 pages, 2007)

130. T. Melo, S. Nickel, F. Saldanha da Gama
Facility Location and Supply Chain Management – A comprehensive review
Keywords: facility location, supply chain management, network design
(54 pages, 2007)

131. T. Hanne, T. Melo, S. Nickel
Bringing robustness to patient flow management through optimized patient transports in hospitals
Keywords: Dial-a-Ride problem, online problem, case study, tabu search, hospital logistics
(23 pages, 2007)

132. R. Ewing, O. Iliev, R. Lazarov, I. Rybak, J. Willems
An efficient approach for upscaling properties of composite materials with high contrast of coefficients
Keywords: effective heat conductivity, permeability of fractured porous media, numerical upscaling, fibrous insulation materials, metal foams
(16 pages, 2008)

133. S. Gelareh, S. Nickel
New approaches to hub location problems in public transport planning
Keywords: integer programming, hub location, transportation, decomposition, heuristic
(25 pages, 2008)

134. G. Thömmes, J. Becker, M. Junk, A. K. Vaikuntam, D. Kehrwald, A. Klar, K. Steiner, A. Wiegmann
A Lattice Boltzmann Method for immiscible multiphase flow simulations using the Level Set Method
Keywords: Lattice Boltzmann method, Level Set method, free surface, multiphase flow
(28 pages, 2008)

135. J. Orlik
Homogenization in elasto-plasticity
Keywords: multiscale structures, asymptotic homogenization, nonlinear energy
(40 pages, 2008)

136. J. Almquist, H. Schmidt, P. Lang, J. Deitmer, M. Jirstrand, D. Prätzel-Wolters, H. Becker
Determination of interaction between MCT1 and CAII via a mathematical and physiological approach
Keywords: mathematical modeling; model reduction; electrophysiology; pH-sensitive microelectrodes; proton antenna
(20 pages, 2008)

Status quo: February 2008